Journal of the Serbian Society for Computational Mechanics / Vol. 15 / No. 2, 2021 / pp 23-31
(10.24874/jsscm.2021.15.02.03)

CORONARY ATHEROSCLEROSIS ASSESSMENT: A NEW ANATOMICAL, FUNCTIONAL, MORPHOLOGICAL AND BIO-MECHANICAL APPROACH

Panagiotis K. Siogkas[1], Georgios-Eleftherios Kalykakis[1], Constantinos D. Anagnostopoulos[2], Themis P. Exarchos[1*]

[1] Department of Informatics, Ionian University, Corfu, Greece
e-mail: psiogkas4454@gmail.com, c18kaly@ionio.gr, exarchos@ionio.gr
[2] Biomedical Research Foundation of Academy of Athens, Athens, Greece
e-mail: cdanagnostopoulos@bioacademy.gr
**corresponding author*

Abstract

The aims of this work are to investigate and compare two different flow dynamics techniques (steady state - pulsatile flow) for endothelial shear stress calculation, compare lesion specific smartFFR and ESS values, as well as total vessel smartFFR and ESS values, and investigate the relationship between smartFFR and ESS to stress MBF (myocardial blood flow) and MFR (myocardial flow reserve). A total of 10 coronary vessels of 6 patients with intermediate pre-test likelihood for coronary artery disease, who have undergone both CTCA and PET-MPI with ^{15}O-water or ^{13}N-ammonia, were included in the study. Seven (7) cases had normal stress MBF and MFR values and three (3) had abnormal ones. PET was considered abnormal when > 1 contiguous segments showed both stress MBF ≤2.3mL/g/min and MFR ≤2.5 for ^{15}O-water or <1.79 mL/g/min and ≤2.0 for ^{13}N-ammonia, respectively. The ESS at the luminal surface of the artery was calculated as the product of viscosity and the gradient of blood velocity near the vessel wall. To calculate the smartFFR, we performed a transient simulation for each case. We used a pressure of 100 mmHg as a boundary condition at the inlet (i.e. mean human aortic pressure). At the outlet, a flow profile of 4 timesteps with a timestep duration of 0.25 sec was used. In each timestep, a volumetric flow rate of 1, 2, 3 and 4 ml/s are applied as outlet boundary conditions. The cut-off value for a pathological smartFFR is 0.83. There is a difference in total vessel calculated smartFFR results compared to the corresponding values of lesion specific smartFFR (0.88 vs 0.97, p=0.01). For ESS there is a negligible difference between lesion specific and total vessel values (2.22 vs 2.74, p = 0.9). There is a moderate negative correlation between both lesions specific (r = -0.543) and total vessel smartFFR and ESS (r = -0.915). ESS values were higher in vessels where vessel smartFFR was considered abnormal (1.97 vs 5.52, p = 0.01). Total vessel length smartFFR was lower in vessels with abnormal PET-MPI compared to the normal vessels (0.75 vs 0.93, p = 0.01). ESS is higher in vessels with pathological stress MBF and CFR (5.5 vs 2.0, p = 0.02). The total vessel length smartFFR and lesion ESS appear to assess the functional significance of the vessel well, when compared to the PET-MPI measurements.

Keywords: smartFFR, atherosclerosis, functional assessment, endothelial shear stress

1. Introduction

The death toll caused by cardiovascular diseases continues to follow a steadily growing rate mainly due to the Westernized method of living, consisting mainly of a total lack of exercise and high-fat diets that include large quantities of red meat which, in turn, cause elevated blood pressure (WHO, 2019).

To counter this increase in mortality, the field of interventional cardiology is constantly expanding and growing. In clinical practice, a variety of coronary imaging techniques are used on a regular basis, including either invasive (i.e. Invasive Coronary Angiography-ICA) or non-invasive techniques (i.e. Computed Tomography Coronary Angiography-CTCA). CTCA has gained traction in recent years because it has the ability to provide details on the structure of atheromatic plaques on both the lumen and the exterior surface. The well-established Fractional Flow Reserve (FFR) technique is used to determine the functional state of a major coronary vessel when the clinician does not have a clear view of the vessel of concern using the aforementioned imaging modalities or when the decision on the treatment that must be pursued is marginal. The procedure is as follows.

The intravascular pressure after the desired stenosis is measured using a dedicated pressure wire and is defined as the ratio of the pressure after the stenosis of interest divided by the mean aortic pressure. The calculation is performed following the patient's medication induction of hyperemia.

Advances in computer science and image processing have enabled the development of three-dimensional reconstruction techniques that can be used in the entire coronary vasculature. Several techniques for 3D reconstruction in the literature that could only use a single imaging model or a fusion of two imaging modalities were published. In recent years, single imaging methods such as CTCA or ICA (De Bruyne et al. 2014; Athanasiou et al. 2016) have been more than adequate for generating either the lumen or any coronary vasculature function, including the entire coronary arterial tree.

The application of computational fluid dynamics (CFD) to 3D coronary models has resulted in the precise and thorough measurement of important hemodynamic variables such as endothelial shear stress (ESS) and smartFFR which is a CT-FFR surrogate (Katritsis et al. 2014; Tang et al. 2020; Tesche et al. 2017) The ESS is a hemodynamic parameter that is highly influenced by vessel geometrical changes (i.e. plaque progression stenosis etc.). This sensitivity is critical for assessing the coronary lesion.

Currently, there are only a few studies investigating the complex relationship between anatomo-morphological and biomechanical data and myocardial blood flow (MBF). Positron Emission Tomography (PET), the gold standard in this area, can be used to accurately calculate the latter (Li et al., 2018; Evans et al., 2016).

Our study's objectives focus mainly on investigating and comparing two different flow dynamics approaches (steady state vs. pulsatile flow) for the endothelial shear stress calculation, on comparing lesion-specific as well as total vessel smartFFR and ESS values, and on investigating the relationship between ESS and smartFFR in addition to myocardial blood flow stress (MBF) and myocardial flow reserve (MFR).

2. Methods

2.1 Study population

Six patients, enrolled in the EVINCI (Neglia et al., 2015) and SMARTooL projects, having undergone CTCA and Positron Emission tomography Myocardial Perfusion imaging (PET-MPI) using ^{15}O-water or ^{13}N-ammonia, with intermediate pre-test likelihood of coronary artery disease (CAD), were included in the study. Details on the imaging procedures and the characteristics of the study population are reported in another study (Neglia et al. 2015). Ethical approval was provided by each participating center and informed consent was obtained by all study participants, as mandated from the main EVINCI study (Neglia et al. 2015).

2.2 3D coronary artery reconstruction

The 3D reconstruction algorithm follows the workflow presented below: a) Pre-processing of the CCTA images with the Frangi Vesselness filter in order to find possible vessel regions. b) Using a minimum cost path approach, the 3D centerline of the vessels is then extracted. c) Employing a membership function of Hounsfield Units (HU) values, an estimation of the weight function for lumen, outer wall, and calcified plaque is made. d) Active contour model estimation segmentation is implemented for the lumen and the outer wall. e) Regarding plaque segmentation, a level set method is applied. f) the 3D surfaces for the lumen, outer wall, and calcified plaques are created. The SMARTool software (Version 0.9.17) was used for the 3D coronary artery reconstruction (Sakellarios et al. 2017).

2.3 Computational fluid dynamics and boundary conditions

The finite element method was used to solve the incompressible Navier-Stokes and continuity equations. A mesh of tetrahedral elements of the same size was created for each vessel and steady state flow simulations were performed. The Navier-Stokes and continuity equations are presented below:

$$\rho \frac{\partial \mathbf{v}}{\partial t} + \rho(\mathbf{v} \bullet \nabla)\mathbf{v} - \nabla \bullet \boldsymbol{\tau} = 0 \tag{1}$$

$$\nabla \bullet (\rho \mathbf{v}) = 0 \tag{2}$$

where $\mathbf{v}$ is the blood velocity vector and $\boldsymbol{\tau}$ is the stress tensor, which is defined as:

$$\boldsymbol{\tau} = -p\delta_{ij} + 2\mu\varepsilon_{ij} \tag{3}$$

where δ_{ij} is the Kronecker delta, μ is the blood dynamic viscosity, p is the blood pressure and ε_{ij} is the strain tensor calculated as:

$$\varepsilon_{ij} = \frac{1}{2}\left(\nabla \mathbf{v} + \nabla \mathbf{v}^T\right) \tag{4}$$

Blood was considered Newtonian, with a density of 1050 kg/m^3 and a dynamic viscosity of 0.0035 Pa·s. Flow was considered laminar and incompressible. The wall was considered to be rigid and a no-slip and no-penetration boundary condition was applied [Evans *et al*., 2016]. We used a pressure of 100 mmHg as a boundary condition at the inlet (i.e., mean human aortic pressure) and the ICA extracted flow for the outlet. Simulations were carried out using a finite element commercial software (ANSYS CFX 15, Canonsburg, PA, USA).

2.4 Assessment of endothelial shear stress

The ESS of the artery was calculated as the product of the viscosity and the gradient of blood velocity near the vessel wall at the luminal surface. ESS was calculated at the area of maximum stenosis as well as in the total vessel length.

2.5 Calculation of smartFFR

Transient simulation was performed for every vessel on order to calculate the smartFFR index. A pressure of 100 mmHg was applied as a boundary condition at the inlet (i.e. mean human aortic pressure) and at the outlet, a flow profile of 5 timesteps with a timestep duration of 0.25 sec was used. In each timestep, a volumetric flow rate of 0, 1, 2, 3 and 4 ml/s are applied as outlet boundary conditions. The wall was assumed to solid without penetration and a no-slip condition was also applied. In order to build the patient-specific P_d/P_a curve, we calculated the P_d/P_a value for every timestep of the simulation and the final values are then plotted and fitted by a smoothing spline consisting of 100 points. The final curve is then used to calculate the area under it, which is then normalized by dividing with the area of the same artery if a healthy vessel was present (Siogkas et al., 2021). The calculated ratio represents the smartFFR value. Based on previous studies (Siogkas et al., 2021) it is considered that the cut off value for a pathological smartFFR is 0.85.

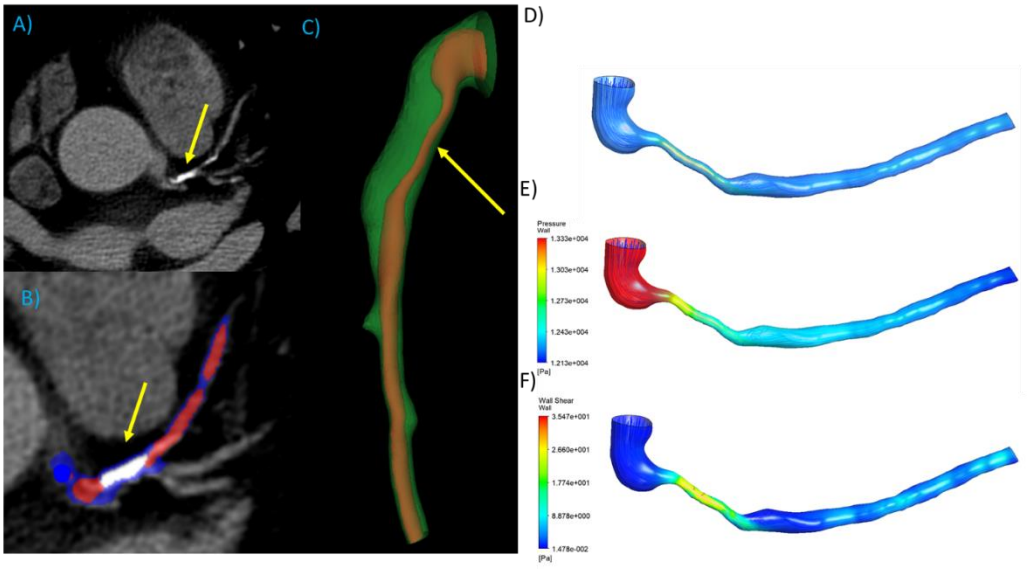

Fig. 1. A) Computed tomography Coronary angiography presenting LAD segment with >70% stenosis severity due to high calcified volume; B) Close up of segment after the lumen(red) and wall (blue) segmentation; C) 3D result presenting the lumen (red) and wall (green); D) CFD flow velocity calculations in the 3D reconstructed model E) SmartFFR calculation; F) ESS calculation.

2.6 PET imaging and data analysis

PET/CT imaging was performed according to international guidelines and the EVINCI study protocol using ^{15}O-water or ^{13}N-ammonia. PET was considered abnormal when >1 contiguous segments showed both stress MBF ≤2.3mL/g/min and Myocardial Flow Reserve (MFR) ≤2.5 for ^{15}O-water or <1.79 mL/g/min and ≤2.0 for ^{13}N-ammonia respectively (Danad et al., 2014).

3. Statistical analysis

Continuous variables are presented as mean values ± SD or median and interquartile range (IQ), while qualitative variables as absolute and relative frequencies. Probability values are two-sided from the t-test and the Mann–Whitney U test for continuous variables. ANOVA or Kruskal–Walli's test was selected for multiple groups comparisons. To compare the two ESS calculation methods, Bland and Altman plots were implemented. A p-value <0.05 was considered statistically significant.

4. Results

4.1 Patient and vessel characteristics

Demographics, clinical and coronary lesion characteristics of the total study population are presented in Table 1. Ten vessels in total were selected. Three consist of abnormal PET-MPI and seven with normal PET-MPI values.

PATIENTS CHARACTERISTICS

Patients (n=6)	N (%)
Age (years)	63.5 ± 3.1
Gender (male)	5(84)
Vessel	
LAD	6(60)
RCA	4(40)
Position of the lesion	
Proximal	8(80)
Middle	2(20)

Table 1. Baseline patients' characteristics.

4.2. Comparison of lesion specific and vessel smartFFR and endothelial shear stress values

Median ESS values present no difference in comparison of lesion specific and total vessel volumes (2.22 vs 2.74, p = 0.9, Figure 2 A). SmartFFR presents a significant difference when calculated in the total vessel compared to the specific lesion (0.88 vs 0.97, p=0.01, Figure 2 B)

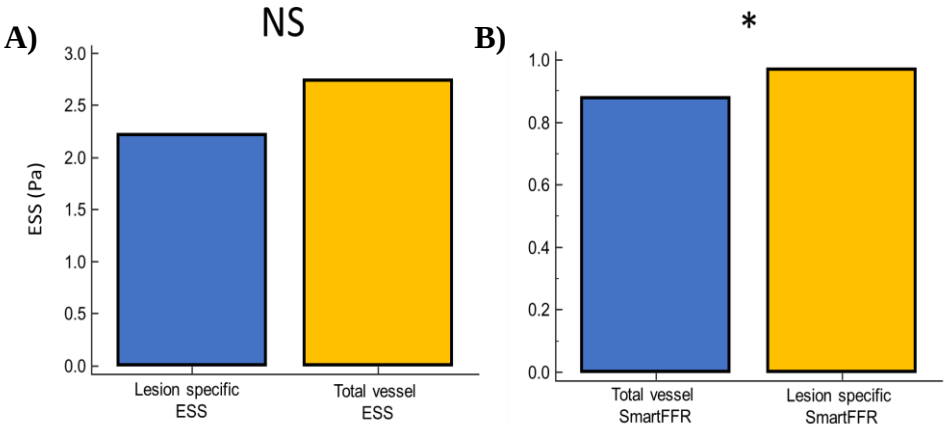

Fig. 2. A) ESS and B) smartFFR values comparison between lesion specific areas and total vessel area.

4.3 Relationship between smartFFR and ESS

There is a moderate negative to high correlation between both lesions specific (r = -0.543, Figure 3 A) and total vessel SmartFFR and ESS (r = -0.915, Figure 3 B) and ESS values were higher in vessels where vessel SmartFFR was considered abnormal (1.97 vs 5.52, p = 0.01, Figure 3 C)

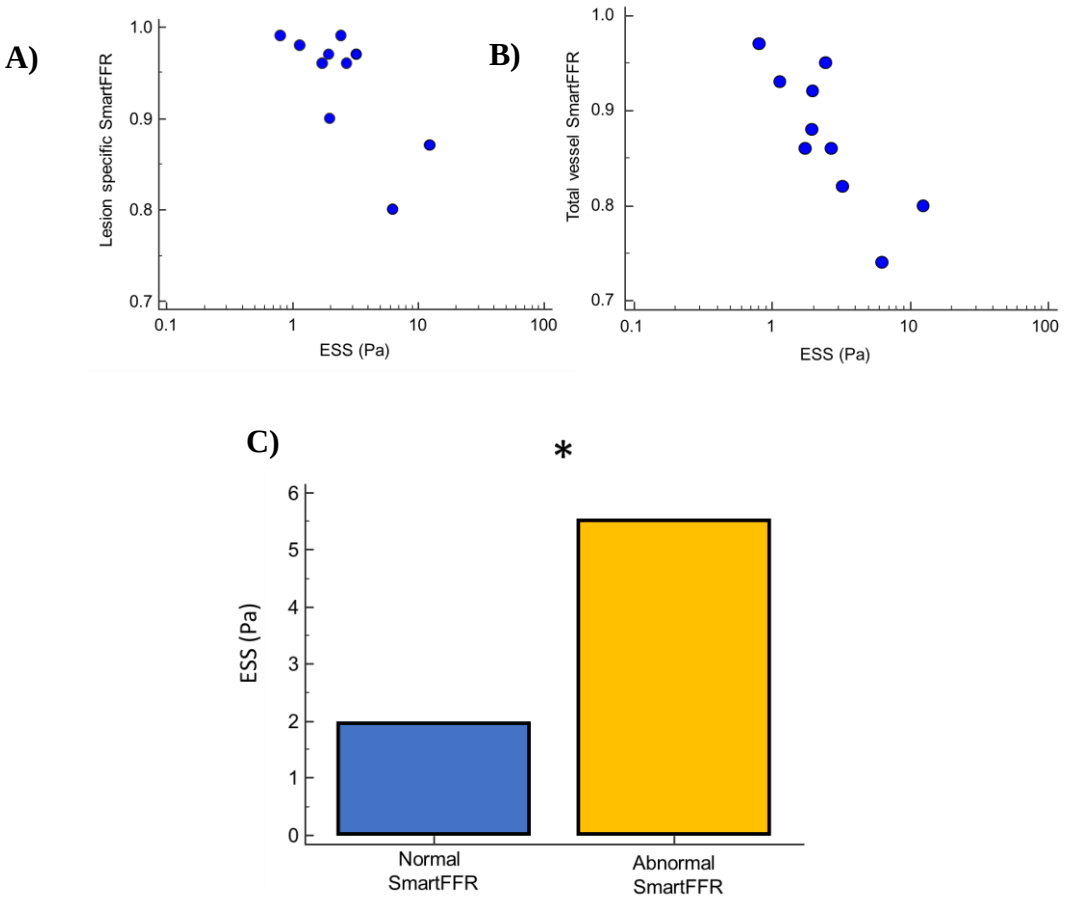

Fig. 3. A-B) Correlation plot between ESS and smartFFR, .C) ESS values in vessels with smartFFR above and below 0.85.

4.4 MBF stress and MFR relationship with smartFFR and ESS

When the PET-MPI results in every vessel is considered, total Vessel length SmartFFR was lower in vessels with abnormal PET-MPI compared to the normal vessels (0.75 vs 0.93, p = 0.01, Figure 4 A). ESS is higher in vessels with pathological MBF stress and CFR (5.5 vs 2.0, p = 0.02, Figure 4 B)

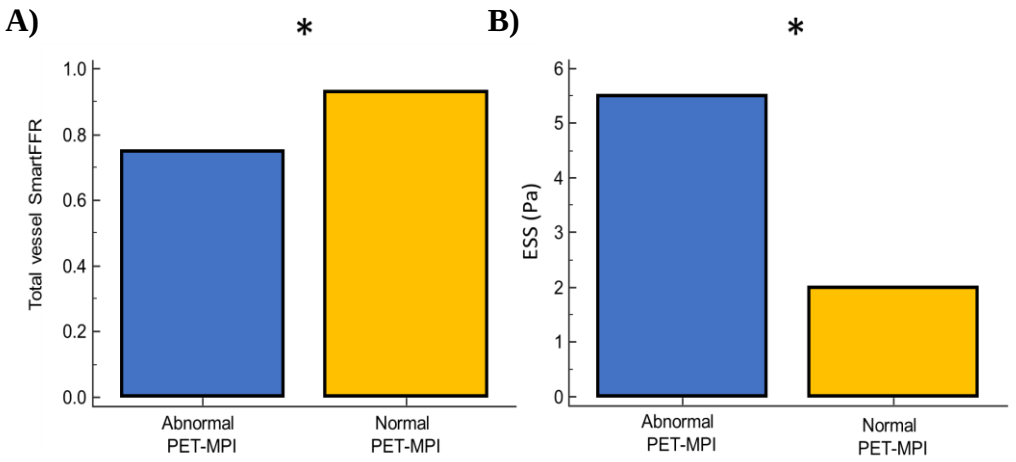

Fig. 4. A) Total vessel SmartFFR in vessels with normal-abnormal PET-MPI; B Lesion specific ESS in vessels with normal-abnormal PET-MPI.

5. Discussion

In this work, we presented a parametric study on how the type of simulation affects the calculation of important hemodynamic parameters and used ten coronary arterial segments with mild or severe stenoses in order to reveal the correlation between hemodynamic parameters such as ESS and smartFFR and PET-MPI derived parameters such as stress MBF and MFR. The main objective of our work was to develop a non-invasive method of the functional assessment of major coronary vessels by combining an already established 3D reconstruction method and a validated FFR surrogate. Higher smartFFR values are present in lesion specific segment compared to the total vessel ones, revealing that the different evaluation approach of a vessel may affect the final clinical result. A pathological, in terms of smartFFR thresholds, lesion may present normal smartFFR values and a normal PET result downstream when using the total lesion length. On the other hand, ESS does not present a difference when calculated at the lesion and the total length of the vessel, due to the fact that it is generally considered a local applied variable and is harder to be determined in great length due to dilution of the values. Negative moderate to high correlation between ESS and smartFFR was observed. This is an important finding that presents the different flow characteristics of a vessel and their ability to present valuable information as separate markers for the flow capabilities of the vessel. Having this in mind, our results presented with a good agreement between the calculated abnormal ESS or smartFFR cases, and the calculated abnormal PET-MPI markers. However, due to the modest dataset size, we cannot end up to safe conclusions regarding the overall efficacy of the proposed combined surrogate marker, thus indicating the need for a more extended validation strategy.

Acknowledgement: This research is co-financed by Greece and the European Union (European Social Fund-ESF) through the Operational Programme «Human Resources Development, Education and Lifelong Learning 2014-2020» in the context of the project “Assessment of coronary atherosclerosis: a new complete, anatomo-functional, morphological and biomechanical approach”, Project number 5047761.

References

Athanasiou L. et al (2016). Three-dimensional reconstruction of coronary arteries and plaque morphology using CT angiography - comparison and registration with IVUS, *BMC Med. Imaging*, vol. 16, no. 1, 2016, doi: 10.1186/s12880-016-0111-6.

Danad I. et al. (2014). Quantitative assessment of myocardial perfusion in the detection of significant coronary artery disease: Cutoff values and diagnostic accuracy of quantitative [15O]H2O PET imaging, *J. Am. Coll. Cardiol.*, vol. 64, no. 14, pp. 1464–1475, doi: 10.1016/j.jacc.2014.05.069

De Bruyne B *et al.* (2014). Fractional Flow Reserve–Guided PCI for Stable Coronary Artery Disease, *N. Engl. J. Med.*, vol. 371, no. 13, pp. 1208–1217, doi: 10.1056/nejmoa1408758.

Evans N. R., J. M. Tarkin, M. M. Chowdhury, E. A. Warburton, and J. H. F. Rudd (2016). PET Imaging of Atherosclerotic Disease: Advancing Plaque Assessment from Anatomy to Pathophysiology, *Curr. Atheroscler. Rep.*, vol. 18, no. 6, June, doi: 10.1007/s11883-016-0584-3.

Katritsis D. and I. Pantos (2014) Fractional flow reserve derived from coronary imaging and computational fluid dynamics, *Interv. Cardiol. Rev.*, vol. 9, no. 3, pp. 145–150, doi: 10.15420/icr.2014.9.3.145.

Li L. et al. (2018). Sodium-fluoride PET-CT for the non-invasive evaluation of coronary plaques in symptomatic patients with coronary artery disease: a cross-correlation study with intravascular ultrasound, *Eur. J. Nucl. Med. Mol. Imaging*, vol. 45, no. 12, pp. 2181–2189, Nov. doi: 10.1007/s00259-018-4122-0.

Neglia D. et al. (2015). Detection of Significant Coronary Artery Disease by Noninvasive Anatomical and Functional Imaging, *Circ. Cardiovasc. Imaging*, vol. 8, no. 3, pp. 1–10, 2015, doi: 10.1161/CIRCIMAGING.114.002179.

Sakellarios A. I. et al. (2017). SMARTool: A tool for clinical decision support for the management of patients with coronary artery disease based on modeling of atherosclerotic plaque process, in *Proceedings of the Annual International Conference of the IEEE Engineering in Medicine and Biology Society, EMBS*, pp. 96–99, doi: 10.1109/EMBC.2017.8036771.

Siogkas P. K. et al. (2021). SmartFFR, a New Functional Index of Coronary Stenosis: Comparison With Invasive FFR Data, *Front. Cardiovasc. Med.*, vol. 8, p. 958, Aug. 2021, doi: 10.3389/fcvm.2021.714471.

Tang C. X. et al. (2020). CT FFR for Ischemia-Specific CAD With a New Computational Fluid Dynamics Algorithm: A Chinese Multicenter Study, *JACC Cardiovasc. Imaging*, vol. 13, no. 4, pp. 980–990, Apr. doi: 10.1016/j.jcmg.2019.06.018.

Tesche C. et al. (2017). Coronary CT angiography-derived fractional flow reserve, *Radiology*, vol. 285, no. 1, pp. 17–33, Oct., doi: 10.1148/radiol.2017162641

WHO. (2019). Available: https://www.who.int/health-topics/cardiovascular-diseases/#tab=tab_1. .